CROSS SECTIONS AND DIFFERENTIAL DISTRIBUTIONS FOR VECTOR-BOSON PAIR PRODUCTION IN NNLO QCD

S. KALLWEIT

PRISMA Cluster of Excellence & Institute of Physics, Johannes Gutenberg University, D-55099 Mainz, Germany
Kavli Institute for Theoretical Physics, University of California, Santa Barbara, CA 93106, USA

M. GRAZZINI, M. WIESEMANN

Physik-Institut, Universität Zürich, CH-8057 Zürich, Switzerland

D. RATHLEV

Theory Group, Deutsches Elektronen-Synchrotron (DESY), D-22607 Hamburg, Germany

We review the computations of the next-to-next-to-leading order (NNLO) QCD corrections to vector-boson pair production processes in proton–proton collisions. Our calculations include the leptonic decays of W and Z bosons, consistently taking into account all spin correlations, off-shell effects and non-resonant contributions. For massive vector-boson pairs we show inclusive cross sections, applying the respective mass windows chosen by ATLAS and CMS to define Z bosons from their leptonic decay products, as well as total cross sections for stable bosons. Moreover, we provide samples of differential distributions in fiducial phase-space regions inspired by typical selection cuts used by the LHC experiments. For the wide majority of measurements, the inclusion of NNLO corrections significantly improves the agreement of the Standard Model predictions with data.

1 Introduction

Vector-boson pair production at the Large Hadron Collider (LHC) provides an important test of the electroweak (EW) sector of the Standard Model (SM) at the TeV scale. As these processes are sensitive to the gauge-boson self-interactions, any small deviation in the observed rates or in the kinematical distributions could give a hint towards new physics, which could be modelled on the basis of higher-dimensional operators in the form of anomalous couplings. Vector-boson pair production processes also constitute backgrounds in many direct new-physics searches, and in Higgs-boson studies the neutral final states represent irreducible backgrounds in the respective decay channels $H \to ZZ/W^+W^-/Z\gamma$.

2 Results

All calculations reviewed here have been carried out with MATRIX[a], a new tool that is based on the Monte Carlo program MUNICH[b], interfaced with the OPENLOOPS[c] generator of one-loop scattering amplitudes [1], and includes an automated implementation of the q_T-subtraction [2] and -resummation [3] formalisms. This widely automated framework has already been used, in combination with the two-loop scattering amplitudes of Refs. [4,5], for the calculations of $Z\gamma$ [6,7], $W^{\pm}\gamma$ [7], ZZ [8,9], W^+W^- [10,11] and $W^{\pm}Z$ [12] production at NNLO QCD as well as in the resummed computations of the ZZ and W^+W^- transverse-momentum spectra [13] at NNLL+NNLO.

In Figure 1 we provide predictions for the inclusive ZZ, W^+W^- and $W^{\pm}Z$ cross sections at different orders in QCD perturbation theory for the relevant centre-of-mass energies. All these results are calculated with NNPDF3.0 parton distribution functions (PDFs) [14], and compared to the cross sections determined by ATLAS and CMS from their respective measurements. Our findings are briefly discussed in Sections 2.2–2.4. The histograms in Figures 2–4 are taken from the original publications and thus use the respective input parameters as specified therein.

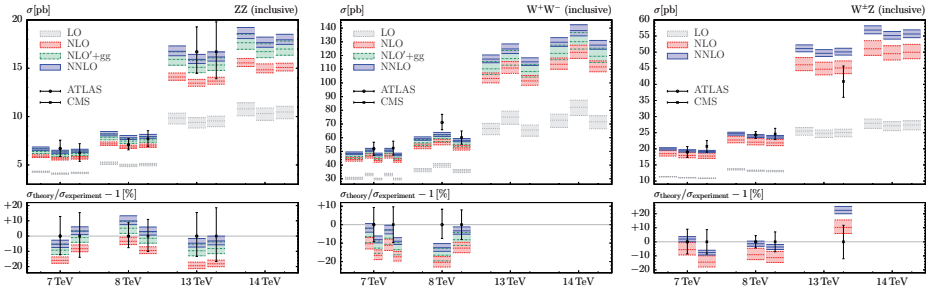

Figure 1 – Total cross sections at LO, NLO, NLO$' + gg$ (NLO plus loop-induced gg contribution, evaluated with NNLO PDFs) and NNLO for ZZ (left), W^+W^- (center) and $W^{\pm}Z$ (right) production, with uncertainties from conventional 7-point scale variations, are shown and compared to experimental results from ATLAS and CMS, where available. For each collider energy, the left column refers to cross sections evaluated with on-shell W and/or Z bosons, while the second (third) column gives fully inclusive off-shell results for four-lepton final states, corrected for their branching ratios, with only mass-window cuts corresponding to the respective ATLAS (CMS) analyses applied. In case of W^+W^- production, the $H \to WW^*$ production cross section predicted in NNLO QCD (from Ref. [11]) is added to the ATLAS predictions for $\sqrt{s} = 8$, 13 and 14 TeV, but not to the CMS predictions, in line with the published experimental setups. At $\sqrt{s} = 7$ TeV results both with (left) and without (right) the Higgs-mediated contribution are shown.

2.1 Fiducial cross sections and differential distributions for $Z\gamma$ and $W^{\pm}\gamma$ production

Measurements of $V\gamma$ final states have been carried out by ATLAS and CMS using the data sets at centre-of-mass energies of 7 TeV [15,16,17] and 8 TeV [18,19]. Due to the massless photon in the final state, a total cross section cannot be defined. Instead, we investigate cross sections in the fiducial phase-space regions chosen by the experiments (see Refs. [6,7]). The higher-order corrections for $W^{\pm}\gamma$ are significantly larger than those for $Z\gamma$: This can be traced back to a suppression of the $W^{\pm}\gamma$ Born contributions due to a *radiation zero*, which is broken only beyond leading order (LO). The loop-induced gluon–gluon contribution to $Z\gamma$ production amounts to

[a] MATRIX is the abbreviation of "MUNICH Automates qT subtraction and Resummation to Integrate X-sections", by M. Grazzini, S. Kallweit, D. Rathlev, and M. Wiesemann. In preparation.

[b] MUNICH is the abbreviation of "MUlti-chaNnel Integrator at Swiss (CH) precision"—an automated parton level NLO generator by S. Kallweit. In preparation.

[c] The OPENLOOPS one-loop generator, by F. Cascioli, J. Lindert, P. Maierhöfer, and S. Pozzorini, is publicly available at http://openloops.hepforge.org.

only about 10% of the $\mathcal{O}(\alpha_s^2)$ corrections. We find significantly larger corrections if the applied selection cuts suppress resonant configurations with the photon emitted from the final-state leptons in Born kinematics. As expected, a jet veto results in a serious reduction of the higher-order effects. The agreement with experimental data is significantly improved, in particular for inclusive $W^\pm\gamma$ production. Figure 2 illustrates these findings by means of the transverse-momentum distribution of the photon in $Z\gamma$ and $W^\pm\gamma$ production.

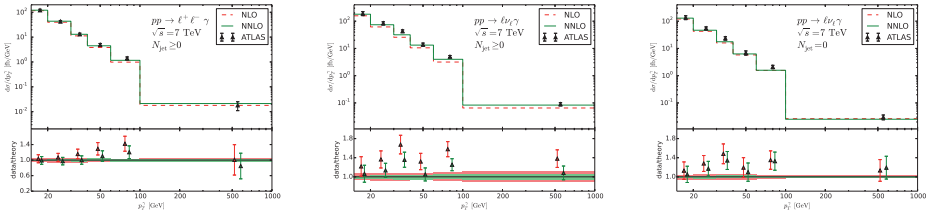

Figure 2 – Distributions in the transverse momentum of the photon in $Z\gamma$ production (left), and in $W^\pm\gamma$ production without (center) and with (right) a jet veto applied are shown, and compared to ATLAS data [15].

2.2 *Inclusive cross sections and normalized differential distributions for ZZ production*

Various measurements of ZZ hadroproduction have been carried out at the LHC by both ATLAS and CMS at 7 TeV [20,21], 8 TeV [22,23] and 13 TeV [24,25], which are in good agreement with NNLO QCD predictions. With typical definitions of fiducial phase-space regions, the higher-order corrections within fiducial cuts [9] mimick those ones found for the fully inclusive results [8] (see Figure 1). The loop-induced gluon–gluon contribution amounts to about 60% of the full $\mathcal{O}(\alpha_s^2)$ corrections. In Figure 3 we show normalized distributions in the four-lepton invariant mass, the leading-lepton p_T and the azimuthal angle between the two reconstructed Z bosons. Due to the large experimental uncertainties, a slightly improved shape agreement can be found only for the last one, which is non-trivial only beyond LO, and thus more affected by the NNLO corrections.

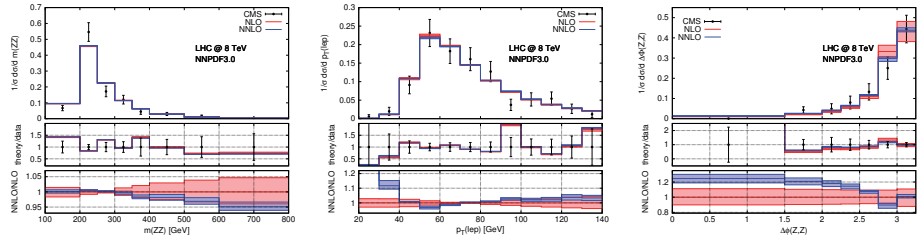

Figure 3 – Normalized distributions in the four-lepton invariant mass (left), the leading-lepton p_T (center) and the azimuthal angle between the two reconstructed Z bosons (right) are shown, and compared to CMS data [23].

2.3 *Inclusive cross sections and differential distributions for W^+W^- production*

The W^+W^- cross section has been measured at the LHC by both ATLAS and CMS at 7 TeV [26,27] and 8 TeV [28,29], agreeing well with the respective SM predictions in NNLO QCD. In order to suppress the enormous background from top-quark pairs, typical fiducial cuts imply a jet veto. Consequently, higher-order effects are quite different for inclusive results [10] (see Figure 1) and predictions within fiducial phase-space regions [11]: Whereas the loop-induced gluon–gluon contribution amounts to only about one third of the $\mathcal{O}(\alpha_s^2)$ effects in the inclusive case, it dominates

if a jet veto is applied, and the genuine corrections to the $q\bar{q}$ channel become even negative. In Figure 4 we show distributions in the dilepton invariant mass, the p_{T} of the dilepton system and the azimuthal angle between the two leptons. By and large the NLO$' + gg$ approximation, which was considered the best prediction before full NNLO results were known, reproduces the NNLO result quite well. However, we find shape distortions of up to about 10% throughout. In phase-space regions that imply the presence of QCD radiation, NLO$' + gg$ cannot approximate the shapes of full NNLO corrections.

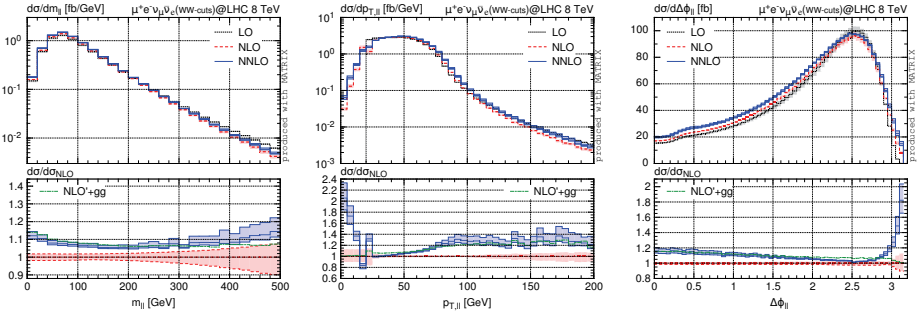

Figure 4 – Distributions in the dilepton invariant mass (left), the p_{T} of the dilepton system (center) and the azimuthal angle between the two leptons (right) are shown. The applied phase-space cuts are inspired by the ATLAS analysis [28], but we do not apply any lepton-isolation criteria with respect to hadronic activity.

2.4 Inclusive cross sections for $W^{\pm}Z$ production

The inclusive $W^{\pm}Z$ cross section has been measured with good precision at the LHC by ATLAS and CMS at centre-of-mass energies of 7 TeV [30,31] and 8 TeV [32,31]. Also an early measurement at 13 TeV [33] by CMS is already available. The agreement with theory predictions is significantly improved by including the recently calculated NNLO corrections [12] (see Figure 1), in particular for LHC Run 1 data. As for $W^{\pm}\gamma$ production, the large corrections are explained by a *radiation zero*, here in the leading helicity amplitudes at Born level, which is overcome only beyond LO.

Acknowledgments

This research was supported in part by the Swiss National Science Foundation (SNF) under contracts 200020-141360, 200021-156585, CRSII2-141847, BSCGI0-157722 and PP00P2-153027, and by the Kavli Institute for Theoretical Physics through the National Science Foundation's Grant No. NSF PHY11-25915.

References

1. F. Cascioli et al., Phys.Rev.Lett. **108** (2012) 111601, [arXiv:1111.5206].
2. S. Catani and M. Grazzini, Phys.Rev.Lett. **98** (2007) 222002, [hep-ph/0703012].
3. G. Bozzi et al., Nucl.Phys. **B737** (2006) 73–120, [hep-ph/0508068].
4. T. Gehrmann and L. Tancredi, JHEP **02** (2012) 004, [arXiv:1112.1531].
5. T. Gehrmann et al., JHEP **09** (2015) 128, [arXiv:1503.04812].
6. M. Grazzini et al., Phys.Lett. **B731** (2014) 204–207, [arXiv:1309.7000].
7. M. Grazzini et al., JHEP **07** (2015) 085, [arXiv:1504.01330].
8. F. Cascioli et al., Phys.Lett. **B735** (2014) 311–313, [arXiv:1405.2219].
9. M. Grazzini et al., Phys. Lett. **B750** (2015) 407–410, [arXiv:1507.06257].
10. T. Gehrmann et al., Phys.Rev.Lett. **113** (2014) 212001, [arXiv:1408.5243].

11. M. Grazzini et al., arXiv:1605.02716.
12. M. Grazzini et al., arXiv:1604.08576.
13. M. Grazzini et al., JHEP **08** (2015) 154, [arXiv:1507.02565].
14. **NNPDF** Collaboration, R. D. Ball et al., JHEP **1504** (2015) 040, [arXiv:1410.8849].
15. **ATLAS** Collaboration, Phys. Rev. **D87** (2013), no. 11 112003, [arXiv:1302.1283]. [Erratum: Phys. Rev.D91,no.11,119901(2015)].
16. **CMS** Collaboration, Phys. Rev. **D89** (2014), no. 9 092005, [arXiv:1308.6832].
17. **CMS** Collaboration, JHEP **10** (2013) 164, [arXiv:1309.1117].
18. **ATLAS** Collaboration, arXiv:1604.05232.
19. **CMS** Collaboration, JHEP **04** (2015) 164, [arXiv:1502.05664].
20. **ATLAS** Collaboration, JHEP **03** (2013) 128, [arXiv:1211.6096].
21. **CMS** Collaboration, JHEP **01** (2013) 063, [arXiv:1211.4890].
22. **ATLAS** Collaboration, ATLAS-CONF-2013-020.
23. **CMS** Collaboration, Phys. Lett. **B740** (2015) 250–272, [arXiv:1406.0113].
24. **ATLAS** Collaboration, Phys. Rev. Lett. **116** (2016), no. 10 101801, [arXiv:1512.05314].
25. **CMS** Collaboration, CMS-PAS-SMP-16-001.
26. **ATLAS** Collaboration, Phys.Rev. **D87** (2013), no. 11 112001, [arXiv:1210.2979].
27. **CMS** Collaboration, Eur. Phys. J. **C73** (2013), no. 10 2610, [arXiv:1306.1126].
28. **ATLAS** Collaboration, arXiv:1603.01702.
29. **CMS** Collaboration, arXiv:1507.03268.
30. **ATLAS** Collaboration, Eur. Phys. J. **C72** (2012) 2173, [arXiv:1208.1390].
31. **CMS** Collaboration, CMS-PAS-SMP-12-006.
32. **ATLAS** Collaboration, Phys. Rev. **D93** (2016) 092004, [arXiv:1603.02151].
33. **CMS** Collaboration, CMS-PAS-SMP-16-002.


LA THUILE
50
22
36
37
6
8
7
54
23
20
52
4
13
27
30
45
48